NISS

Permeability and Healing of Cracked Concrete

Corina-Maria Aldea, Surendra P. Shah,
and Alan F. Karr

Technical Report Number 76
March, 1998

National Institute of Statistical Sciences
19 T. W. Alexander Drive
PO Box 14006
Research Triangle Park, NC 27709-4006
www.niss.org

PERMEABILITY AND HEALING OF CRACKED CONCRETE

By Corina-Maria Aldea, Surendra P. Shah and Alan Karr

ABSTRACT

The goal of the research presented here was to study the relationship between cracking and water permeability. A feedback-controlled test was used to generate width-controlled cracks. Water permeability was evaluated by a low-pressure water permeability test. The factors chosen for the experimental design were material type (paste, mortar, normal and high strength concrete), thickness of the sample and average width of the induced cracks (ranging from 50 to 350 microns). The water permeability test results indicated that the relationships between permeability and material type differ for uncracked and cracked material, and that there was little thickness effect. Permeability of uncracked material decreased from paste, mortar, normal strength concrete (NSC) to high strength concrete (HSC). Water permeability of cracked material significantly increased with increasing crack width. For cracks above 100 microns, NSC showed the highest permeability coefficient, where as mortar showed the lowest one. The permeability of cracked specimens decreased significantly with time. One-sided attenuation measurement indicated the possibility of autogenous healing of cracks.

KEYWORDS

attenuation of the signal, autogenous healing, crack width, crack opening displacement (COD), cumulative flow, damage, feedback-controlled test, flow rate, microcracks, nondestructive evaluation, permeability coefficient, permeation curve, recovery, self-sealing, splitting tensile test, water permeability.

INTRODUCTION

Permeability of concrete plays a critical role in controlling the properties of concrete and the performance of concrete structures. In particular durability of concrete and the corrosion of reinforcing steel are intimately linked to the water permeability of exposed concrete surfaces, like pavements and bridge decks. Cracks that may form, whatever their origin (mechanical, thermal, physico-chemical etc), can act as major pathways for water or aggressive chemical ions to penetrate in concrete, enabling its deterioration. Knowledge of flow properties both of sound and cracked material is fundamental for predicting its durability, as deterioration mechanisms, such as freezing, corrosion, leaching, depend on the flow of aggressive agents through the material.

A prior permeability study performed at ACBM, Northwestern University introducing feedback-controlled splitting tests to induce width-controlled cracks in concrete specimens was reported earlier [1]. This study pointed out the advantages of using feedback-controlled splitting tests to obtain a series of specimens with different crack widths, and evaluated water permeability of concrete with different crack widths. Water permeability proved dependent on the value of the crack opening in the concrete.

Gerard et al. [3], [4] studied the increase in permeability resulting from mechanically-induced cracking. Normal and high concrete samples were subjected to uniaxial tension, and the water permeability was measured in a direction perpendicular to the axis of loading through open cracks having widths ranging from 0.1 to 100 microns. The experimental results showed that permeability of cracked concrete cannot be correlated with that measured on the uncracked material and that the permeability of the specimens is strongly dependent upon the crack width.

In the current study a number of factors which may influence the relationship between crack width and permeability were examined. These include: thickness of the sample,

material composition (paste, mortar, normal strength concrete and high strength concrete), and the average width of the crack. Cracks of designed widths were induced in the concrete specimens using feedback controlled splitting tensile test. Water permeability of cracked concrete was then evaluated by a low pressure water permeability test. Results suggest that among the considered parameters, material type and crack parameters significantly affect water permeability. Long-term permeability showed a decrease over time due to the ability of concrete to seal itself over time. One-sided stress wave attenuation measurements proved to be a potential method to quantify autogenous healing of cracks. Other mechanisms at the microstructural level and crack characteristics need to be investigated in order to properly correlate crack width to water permeability. The results of the present study can be used in a design phase of a structure or in the repairs of crack formation in existing construction.

EXPERIMENTAL PROGRAM

Test Series and Mix Proportions

Table 1 presents the details of mix ingredients and their proportions. Compressive and tensile strengths and modulus of elasticity were measured at 28 days (Table 2). Test series included (1) paste (PASTE), (2) mortar (MORTAR), (3) normal strength concrete (NSC) and (4) high strength concrete (HSC). Cylindrical molds 100 x 200 mm (4 x 8 in) were used for casting. Cylinders were demolded after 24 hours and then stored in a controlled chamber, at 20° C and 100% RH until the age of 28 days. Cylinders were sawn into slices, and then tested. Twenty-five millimeters slice from the top and bottom of each cylinder was cut and discarded. The remaining part was cut into four slices: two 25 mm thick and two 50 mm thick. Samples were soaked in water at room temperature immediately after cutting, as well as in between the tests, in order to avoid drying and any further microcracking. Cutting was performed a day before inducing cracks by means of

the feedback-controlled splitting test, at 28-day age. Then samples were vacuum saturated according to [5] and set up for the water permeability test (WPT).

Experimental Design

Experimental design is indicated on Table 3. Nine levels of crack opening displacement (COD) were assigned to the eighteen samples that were to be produced from each different type of material. Each COD level was then used twice for each material type. Each COD level also appeared the same number of times with a 25 mm (1 in) slice as it does with a 50 mm (2 in) slice. The resulting design produced a balance of all the factor levels against each other and produced a design with as many different types of cracks as possible in the number of samples that could be produced and tested.

Feedback-controlled Test

Feedback-controlled splitting tests were used to induce width-controlled cracks in the specimens (Figure 1). Splitting tensile test (Brazilian test) is one of the methods for estimating the tensile strength of concrete through indirect tension tests. This test was carried out on cylindrical samples, 100 mm (4 in) diameter and 25 mm or 50 mm (1 in or 2 in) thick, tested on their side in diametral compression. Load was applied through plywood strips (25 mm wide and 3 mm thick), interposed between the cylinder and the platens of the testing machine. An infinitesimal element of area located on the vertical diameter is subjected to vertical compression stress and horizontal tensile stress. Stress distribution shows very high compressive stresses near the ends of the vertical diameter, and almost uniform tensile stress over the middle two-thirds of the specimen. Since the concrete is much weaker in tension than in compression, failure occurs in splitting tension at much lower load than would be required to crush the specimen in compression, thus allowing the evaluation of the tensile strength of concrete [6].

The 4.4 MN (one million pound) test machine with a 490 kN strain gage load cell to measure the force was used for the tests. Force calibrated range was different, depending to the test series: 49 kN for PASTE, MORTAR and NSC and 489 kN for HSC. Crack rarely propagates simultaneously from both sides of the cylinder when under load. This suggests that the displacement should be monitored on both sides of the specimen with two transducers, and that the controlled variable has to be the average of their records [7]. A linear variable displacement transducer (LVDT) with a range of 0.5 mm was glued on each side of the slices, normal to the loading direction. Average recorded displacement of the two LVDTs was used as a feedback control. The average crack opening displacement was increased with a constant rate, depending on the material behavior: 0.025 μm/sec for PASTE, 0.12375 μm/sec for MORTAR and 0.25 μm/sec for NSC and HSC. Specimens were loaded under the feedback controlled condition until the average crack reached the desired imposed value, then unloading was performed under force control. Imposed crack openings under loading were 50, 100, 140, 170, 200, 250, 300 and 350 microns. PASTE proved very brittle and extremely difficult to test; consequently the maximum crack opening introduced under loading was limited to 200 microns. Time, load, stroke, lateral displacements on the sides of the sample and their average, called average lateral displacement or average crack opening displacement (COD) were recorded during the test. Tensile stress σ was calculated as:

$$\sigma = \frac{2P}{\pi LD} \tag{1}$$

Where P is the compressive load on the cylinder, L is the length of the cylinder, D is its diameter. Test results were plotted as individual stress versus COD curves for all the slices tested.

Water Permeability Test

Cracked samples were used for the water permeability test, involving: vacuuming and saturation, setting up the test and taking the measurements, as described in [1].

Vacuuming and saturation were performed according to sample preparation suggested for rapid chloride permeability test [7]. Specimens were placed in the vacuum desiccator, pressure was reduced to less than 1 mm Hg (133 MPa), and then maintained for 3 hours. De-aired water was added such as the samples were soaked, and same vacuum level was maintained for another hour. Specimens were soaked in the added water for 18 hours after turning off the pump.

Once removed from the desiccator, the discs were dried on the lateral surface with paper towel and then waterproofed with five-minute-epoxy. The samples were then clamped between two plexiglas rings (7.62 cm in diameter and 2.54 cm thick), each attached to a squared plexiglas plate (13.97 x 13.97 cm, 1.27 cm thick), by means of four threaded bars. A pipette (10 ml x 1/10) was mounted in the top plate in order to monitor the water level, and a U-shaped copper pipe was mounted on the bottom plate, in order to ensure the atmospheric pressure at the bottom level of the sample. In order to better tighten the samples, rubber gaskets (7.62 cm in diameter and 0.22 cm thick) were interposed between the sample and each of the plexiglas rings. After setting up the cell, the lateral surface of the sample and the bottom part of the plastic rings were sealed with silicon rubber in order to avoid any leakage. As soon as the silicon rubber was set, tap water was added in the setup, filling the plastic rings, as well as the pipette and the copper pipe.

Water permeability test (WPT) represents a modified version [1] of a water permeability test developed at the University of Illinois at Urbana-Champaign [2]. The test is a low pressure WPT and consisted in monitoring the water level in the pipette and then refilling it with a syringe at the initial level. During the test only inflow was measured. The whole setup was based on the idea of axial water flow through the sample, due to a low pressure of approximately 30-cm head (Figure 2). The change in head was recorded regularly, the frequency of measurements depended on the material type, the average crack opening after unloading, and the time elapsed after the beginning of the test. Readings were taken once a day for uncracked and small cracks samples, or several times a day for wider cracks at the beginning of the test. Plotting cumulative flow versus time curve indicated a

nonlinear behavior in the beginning, then after some days an almost linear one, as a proof that the flow becomes steady. Some results [2] for uncracked concrete suggest that the nonlinear part of the curve is due to continued saturation, absorbtion of water into the interconnected pores, or continued hydration, which take place for about 7 days. Other investigators [8] assume that steady state flow is reached when outflow equals inflow, that is 8 to 21 days after the beginning of the test. In the literature testing duration varies between 7 [9] and [10], 15 [2] and 21 days [8] for uncracked concrete, and 20 days for cracked concrete [1]. In the present study water permeability was monitored up to 90 to 100 days for all the specimens tested.

In the calculations laminar flow was assumed. Darcy's law was used for the flow through the samples:

$$Q = kA\frac{h}{l} \tag{2}$$

Continuity of flow throughout the system was assumed [11]. The discharge of the pipette is given by:

$$dV = A'\left(\frac{dh}{dt}\right) \tag{3}$$

Where: Q is the rate of flow (Q=dV/dt), V the total volume of water permeated, A the cross sectional area of concrete, t time, h head of water, l thickness of the sample, k permeability coefficient, A' area of the pipette.

The permeability coefficient results combining (2) and (3), after integration:

$$k = \left(\frac{A'l}{At_i}\right)\ln\left(\frac{h_0}{h_i}\right) \tag{4}$$

where t_i is time between two successive readings, h_0, h_i head of water at the beginning, respectively at the end of the test.

DISCUSSION OF RESULTS

Feedback-controlled Test

According to [7] the deformation of concrete subjected to tensile loading increases homogeneously in the beginning and localizes within a planar region that develops as a crack. The region outside the cracks unloads and the crack continues to open in a narrow region, but the crack is not necessarily located in the middle of the specimen. As a consequence of the large unloading region, the load-displacement response exhibits a snap-back.

Typical stress COD curves for the considered materials are plotted in Figure 3. Individual curves exhibited similar trends, and the following can be remarked. A linear part corresponds to loading of the specimen up to the peak load, when the tensile strength of the material is reached. Average lateral displacements corresponding to the peak load ranged from about 9 microns for PASTE and NSC, 12 microns for HSC to 16 microns for MORTAR. As the tensile strength was reached, cracking was initiated, a drop in load and a plateau of almost constant load depending on material type were noticed. The percentage of the peak load in the plateau varied between about 40% for PASTE, 65% for MORTAR and HSC and 80% for NSC. The specimen was unloaded as soon as the designed average lateral displacement was reached. After unloading, the crack widths were reduced by approximately 32 to 75% depending on material type.

The experimental data in the present study confirmed that the crack does not propagate simultaneously from both faces, as stated in [1] and [7]. It was noticed that the crack opened more on one of the faces than on the other one up to the plateau, then the openings became almost the same until the end of the test. This explains why it is necessary to monitor lateral displacement on both sides of the specimen, and that the controlled variable has to be the average of the LVDT readings.

Recovery of crack opening displacement after unloading is presented in Figures 4 and 5. An overall look at the graphs showing the relationship between COD under loading and COD after unloading indicates that all the materials tested exhibit comparable trends. Investigating the influence of the geometry of the specimens (Figure 4), the results suggest that thickness of the samples had little effect upon COD after unloading. However, among the tested materials, results range between MORTAR, which behaved most linearly, and NSC, which behaved most nonlinearly, especially for the thinner specimens. Figure 5 presents the material effect on COD after unloading. Results are almost similar for all the considered material types in the lower range of CODs under loading. However, for wider cracks MORTAR specimens show a higher recovery than NSC. This may be because of the higher tortuosity of cracks in NSC.

Water Permeability Test

Water permeability is commonly quantified by cumulative flow and permeability coefficient. Cumulative flow or permeation curves were plotted based on change in head. Figure 6 indicates that cumulative flow increases with crack opening. According to [2] the slope of the permeation curve is proportional to the permeability coefficient at any time. The curves clearly distinguish a nonlinear behavior in the first days of water permeability test and then a linear behavior, indicating a steady flow. In order to compare the results from this study with the previous work, the permeability coefficient was calculated as an average of permeability coefficients calculated between day 14 and 20. Figure 7 presents a typical permeability coefficient curve in time. Each point in the figure represents an individual permeability coefficient based on equation (4) and corresponding to the time frame between two successive readings.

Good agreement of the results obtained from the present study with the prior study developed at Northwestern University [1] in terms of cracking effect on permeability coefficient is shown by Figure 8. This suggests that in the range of small cracks under

loading, up to about 100 microns, cracking had little effect on concrete permeability, while for crack widths above 100 microns water permeability increased rapidly.

Figure 9 presents material effect on permeability in the same cracking range after unloading. It can be observed that permeability showed dependence on material type. Permeability of uncracked material decreased from PASTE, MORTAR, NSC to HSC, as expected. Cracking changed the material behavior in terms of permeability. For cracks above 100 microns after unloading, NSC showed the highest permeability coefficient, where as MORTAR showed the lowest one. This might have been caused by the difference in morphology of the cracks and by the effect of the transition zone.

Figure 10 presents thickness effect on permeability. Samples with the same crack widths after unloading were selected. It can be observed that although permeability coefficients for the considered thicknesses were not identical, they were however comparable, and thus it can be concluded that thickness had little effect on permeability. MORTAR exhibited the least thickness dependence among the tested materials

Crack Healing

In the present study water permeability was monitored up to 90 to 100 days for all the specimens tested. Water flow decreases with time, and consequently permeability decreases. The decrease in permeability coefficient depends on initial crack opening. Possible reasons for the decrease in flow with time are autogenous healing of cracks, as well as self sealing of uncracked material. Autogenous healing refers to the ability of cement to heal cracks in fractured concrete. Possible reasons are: chemical precipitation of calcium hydroxide and calcium carbonate, mechanical blocking, obstruction of narrow crack areas with ultrafine material, swelling and rehydration of the hardened cement paste on the crack walls. Edvardsen suggests a model for the autogenous healing of cracks as a consequence of calcite formation [12]. Self-sealing refers to the phenomenon of time dependence of flow during a saturated permeability test of uncracked cement-based

material. Hearn concluded that self-sealing was mainly caused by chemical interaction of water with the cement matrix [9], [10].

Monitoring the dependence of permeability coefficient with time, the experimental results available (90 to 100 days) suggest that both cracked and uncracked material exhibit changes in permeability (Figure 11). However, decrease in permeability for uncracked concrete is relatively small. For cracked concrete, depending upon the crack width, permeability decreases by several orders of magnitude. The results of the present research showed that for all the cracked specimens the permeability tended to decrease to the range corresponding to that of the uncracked material. This behavior seems to reveal the ability of material to seal itself in time. This feature proves a potential of improvement of the behavior in service life of concrete exposed to water flow and other related deteriorating mechanisms, and could be deliberately used both in the design of a structure and in the repair of cracks in existing ones. The results from the present study suggested that for cracked concrete it is important to monitor flow until a constant value is reached. The duration of the test depends on cracking level, and both initial and final permeabilities should be recorded.

Investigation of Autogenous Healing Using a Nondestructive Evaluation Technique

The extent of crack healing was investigated using a nondestructive evaluation technique. One-sided stress wave attenuation measurements were used to quantify cracking one day after inducing the crack and then after 100 days of WPT. The technique for wave attenuation measurement was initially developed at Northwestern University to monitor the extent of damage in concrete pavements [13]. The experimental setup is presented in Figure 12. Two recievers were attached with wax to the surface of the specimen and located on each side of the crack, along a diameter perpendicular to the crack. The recievers were miniature accelerometers measuring the out of plane component of acceleration, with sensitivity in the range of 0 to 80 kHz. A solenoid-driven impact source with a frequency content of 0 to 60 kHz was used to produce the waves detected by the

recievers, captured by a digital oscilloscope, and sent to a computer with an interface for data manipulation. The source was located on each side of the crack along a line with the recievers. The spacings betweem the source-reciever and reciever-reciever were 20 mm. The source and recievers locations were marked and kept constant for all the tests performed on each of the samples. Five signals were recorded for each source location. All the signals obtained from the samples showed good repetability in the frequency range of 30 to 60 kHz. Theoretically, attenuation of the signal between the reciveres may vary from 0, complete attenuation, to 1, no attenuation. One-sided attenuation measurement proved sensitive to cracking for all the materials tested (Figure 13). A drastic drop in attenuation value compared to the uncracked material was noticed in case of cracks wider than about 100 microns. Within one geometry and material type, the attenuation measurements clearly distinguish between the magnitude of damage: crack widths below 100 microns and above 100 microns. Attenuation measurements performed after 100 days WPT show a significant change for the cracked samples. The attenuation value increased and became closer to that corresponding to the uncracked sample (Figure 14, dotted line). The recovery in signal suggests filling of cracks. This is probably due to autogenous healing of the cracks. Even without systematic optimization of the test setup, the results appear to have promise in distinguishing damage levels. One-sided attenuation measurement is suggested as a potential method to quantify autogenous healing of cracks.

SUMMARY AND CONCLUSIONS

A. Results of the feedback-controlled splitting tests indicate that

1. The relationship between crack opening displacement (COD) under loading and COD after unloading is comparable for all the materials tested.

2. Material type affects COD after unloading. As the cracks become wider, recovery decreases from NSC, HSC to MORTAR. This might be explained by the

morphology of the cracks going through the material. NSC exhibits probably a more tortuous crack, thus resulting in a less elastic response.

3. Thickness of the samples had little effect upon the relative magnitude of COD after unloading.

B. Results of the water permeability test indicate that:

4. The relationships between permeability and material type differ for uncracked and cracked specimens.

5. Permeability of uncracked material decreased from PASTE, MORTAR, NSC to HSC, as expected.

6. However, in the wider crack range (above 100 microns after unloading), NSC showed the highest permeability coefficient, where as MORTAR showed the lowest value. This might have been caused by the difference in morphology of the cracks and by the effect of the transition zone.

7. Thickness of the samples had little effect upon the permeability coefficient.

5. The permeability of cracked specimens decreased significantly with time. This may be due to autogenous healing.

6. One-sided attenuation measurement indicated the possibility of autogenous healing of cracks.

ACKNOWLEDGEMENTS

This research was carried out at the ACBM Center, Northwestern University. Support from the National Science Foundation (NSF) through grant DMS/9313013 to the National Institute of Statistical Sciences (NISS) is greatly appreciated. Dr. John Popovics and Ph. D. candidate Won-Joon Song are acknowledged for their support and help in performing the one-sided attenuation measurements.

REFERENCES

[1]. Wang, K., Jansen, D., Shah, S.P., Karr, A., Permeability study of cracked concrete, *Cement and Concrete Research*, Vol. **27**, No. 3, pp. 381-393, 1997.

[2]. Ludirdja, D., Berger, R. L., Young, F., Simple Method for Measuring Water Permeability of Concrete, *ACI Materials Journal*, Vol. **86**, No. 5, September-October, pp. 433-439, 1990.

[3]. Gérard, B., Breysse, D., Ammouche, A., Houdusse, O., Didry, O., Cracking and Permeability of Concrete Under Tension, *Materials and Structures*, Vol. 29, April, pp. 141-151, 1996.

[4]. Gérard, B., Marchand, J., Breysse, D., Ammouche, A., Constitutive Law of High-Performance Concrete Under Tensile Strain, 4th International Symposium on Utilization of High-Strength/High-performance Concrete, Paris, 1996.

[5]. Standard Test Method for Electrical Indication of Concrete's Ability to Resist Chloride Ion Penetration, Designation C 1202 – 94, *Annual Book of ASTM Standards, Vol. 04.02*, pp. 620-625.

[6]. Castro-Montero A., Jia Z., Shah S.P., Evaluation of Damage in Brazilian test Using Holographic Interferometry, *ACI Materials Journal*, vol. **92**, No. 3, May-June, pp.268-275, 1995.

[7]. Gettu, R., Mobasher, S., Carmona, S., Jansen, D., Testing of Concrete Under Closed-Loop Control, *Advanced Cement-Based Materials*, Vol. **3**, No. 2, pp.54-71, 1996.

[8]. Ruettgers, A., Vidal, E. N., Wing, S. P., An Investigation of the Permeability of Mass Concrete with particular Reference to Boulder Dam, *Journal of the American Concrete Institute – Proceedings*, March-April, pp. 382-416, 1935.

[9]. Hearn, N., *Saturated Permeability of Concrete as Influenced by Cracking and Self-sealing*, Ph. D. Thesis, University of Cambridge, p. 229, 1992.

[10] Hearn N., Morley C.T., Self-sealing property of concrete – Experimental evidence, *Materials and Structures*, vol. **30**, August-September, pp. 404-411, 1997.

[11]. Cernica, J. N., *Geotechnical Engineering: Soil Mechanics*, John Wiley & Sons, Inc., p. 125, 1995.

[12]. Edvardsen, C., Water Permeability and Autogenous Healing of Separation Cracks in Concrete, *Concrete Precasting Plant and Technology*, vol. **62**, November, pp.77-85, 1996.

[13] Popovics J.S., Song W. and Achenbach, J.D., ``A study of surface wave attenuation measurement for application to pavement characterization," to be published in *Proceedings of the SPIE conference Structural Materials*

Technology: An NDT Conference, Volume 4000, edited by R. Medlock, SPIE, Bellingham Washington, 1998.

LIST OF TABLES

LIST OF FIGURES

Figure 13. One-sided attenuation measurement; cracking effect, NSC, 50 mm.

Figure 14. One-sided attenuation measurement; WPT effect, NSC, 50 mm.

Table 1. **Details of test series and mix proportions.**

Mix Ingredients		Weight by mc of material (kg)			
		PASTE	MORTAR	NSC	HSC
Cement		325.585	155.874	81.905	114.639
Aggregate	# 4	-	-	304.010	286.329
	# 8	-	83.592	43.924	40.904
	# 16	-	33.367	17.536	16.362
	# 30	-	34.125	17.936	16.362
	# 50	-	68.034	35.746	32.723
	# 100	-	33.945	17.802	16.361
Water		146.513	95.878	50.374	25.852
Silica Fume		-	-	-	29.198
Superplasticizer		-	-	-	3.351
W/C		0.45	0.45	0.45	0.31

Table 2. **Material Properties**

Material Properties	Material Type			
	PASTE	MORTAR	NSC	HSC
Slump (cm)	-	-	7.5	1.8
Modulus of Elasticity (GPa)	12.37	18.57	32.14	19.12
Tensile Strength (MPa)	1.57	4.25	3.84	5.69
Compressive Strength (MPa)	55	33	36	69

Table 3. Experimental Design

Factor	Material Type	Thickness (mm)	COD under load (microns)
Level 1	PASTE	25	0 (uncracked)
Level 2	MORTAR	50	50
Level 3	NSC	-	100
Level 4	HSC	-	140
Level 5	-	-	170
Level 6	-	-	200
Level 7	-	-	250
Level 8	-	-	300
Level 9	-	-	350

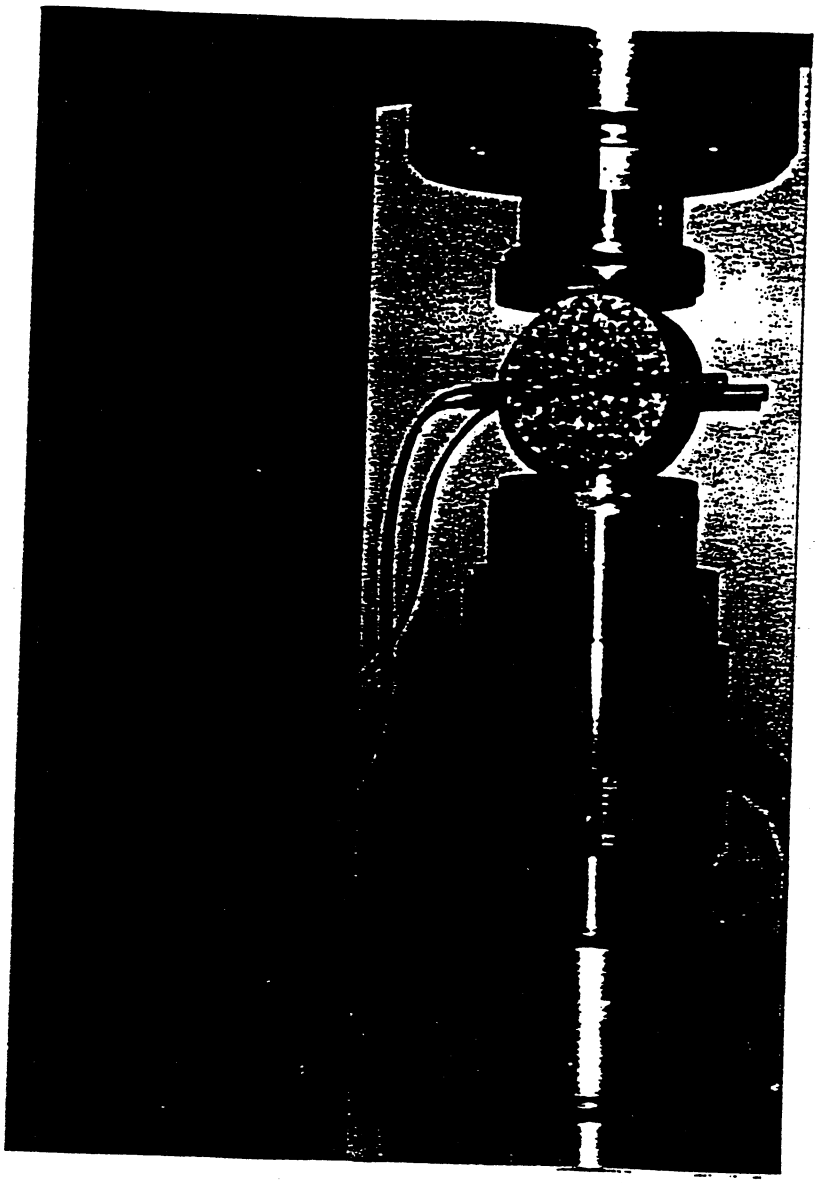

Figure 1. Feedback-controlled splitting test in progress.

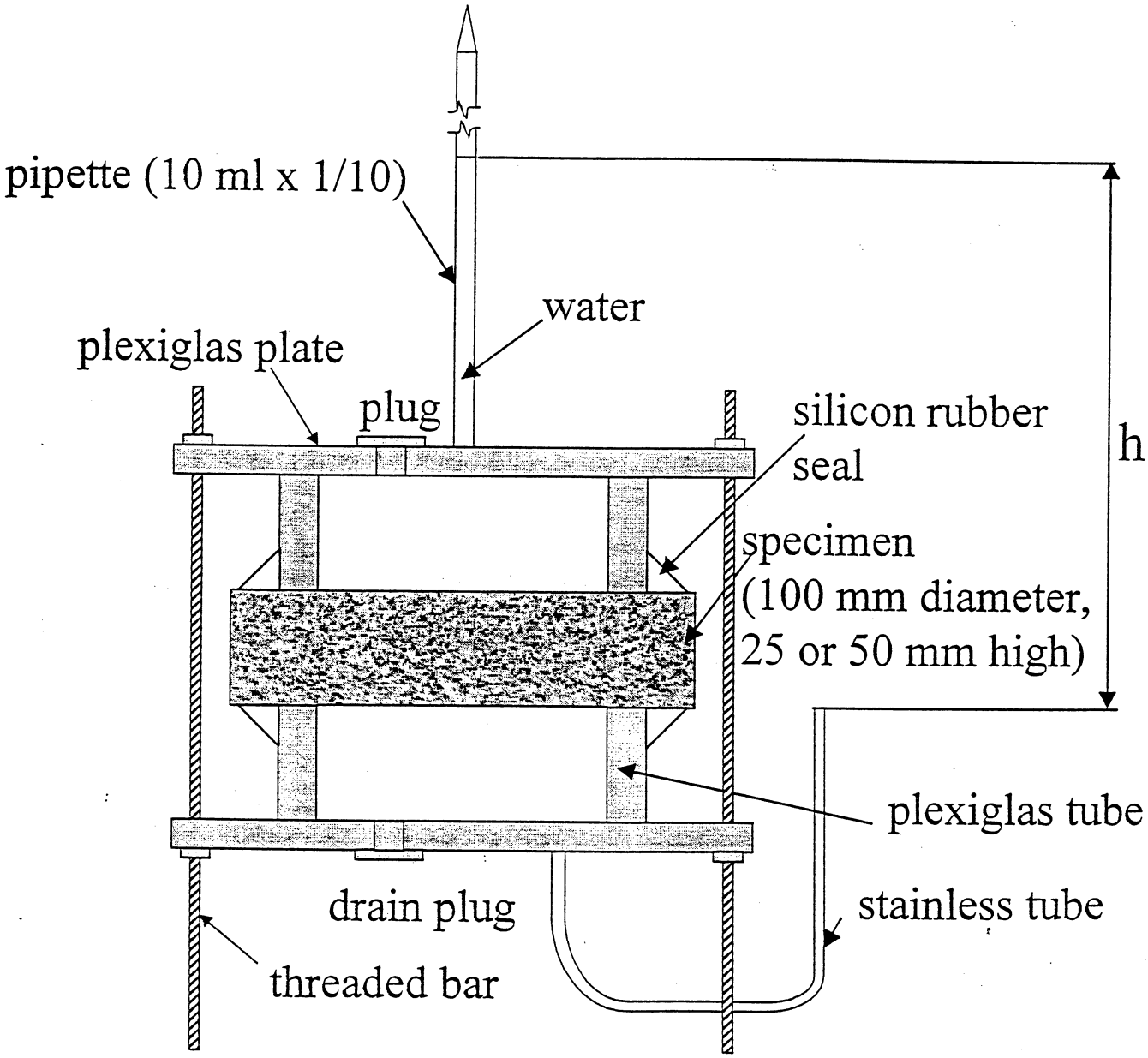

Figure 2. Water permeability test setup.

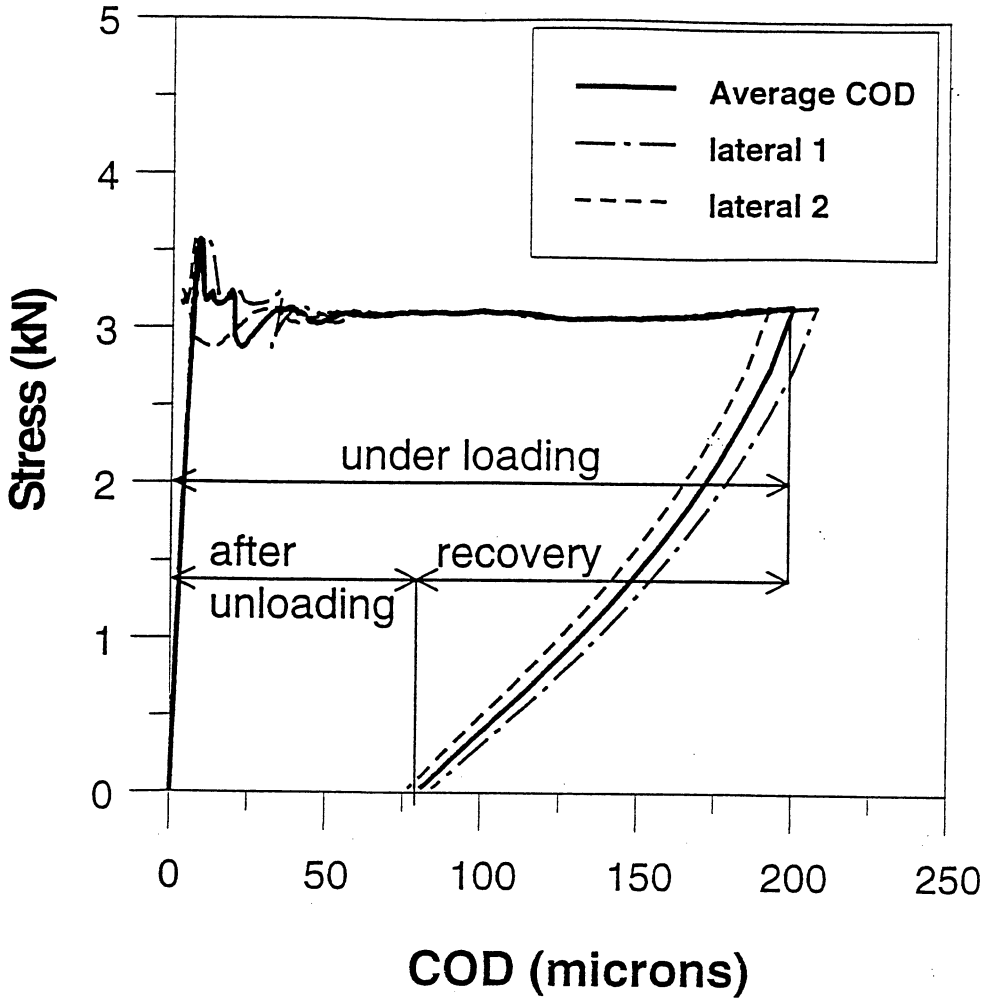

Figure 3. Typical splitting tensile test stress-COD curves. NSC, COD 200 microns.

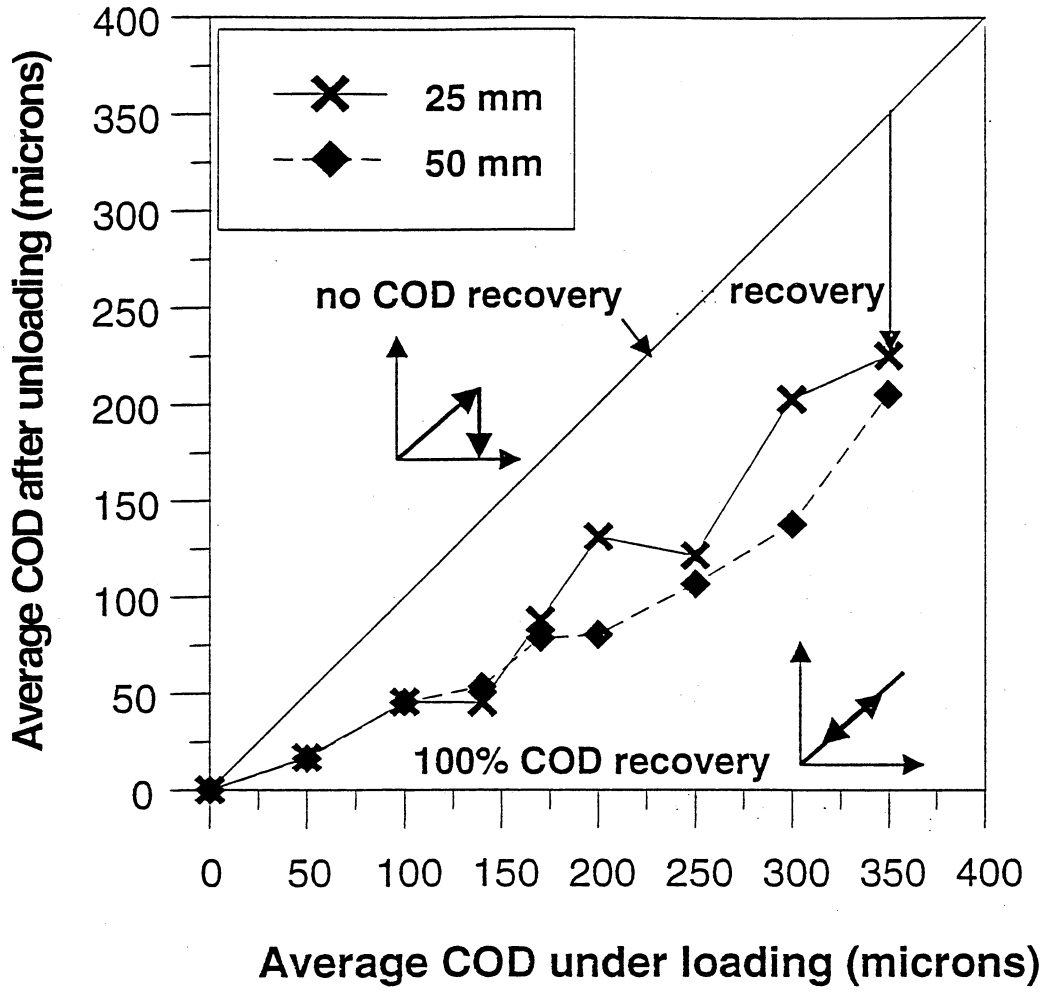

Figure 4. Recovery of COD after unloading. NSC, thickness effect.

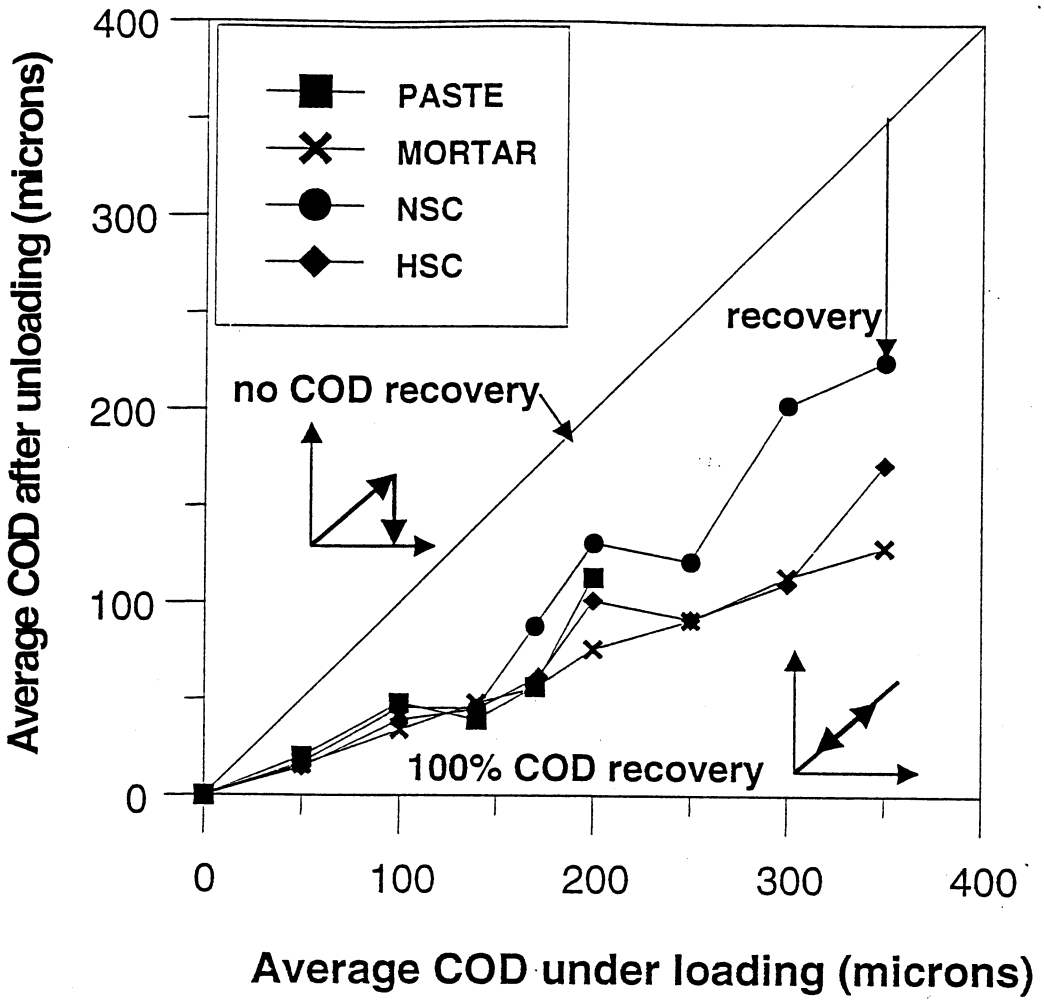

Figure 5. Recovery of COD after unloading. Material effect, 25 mm.

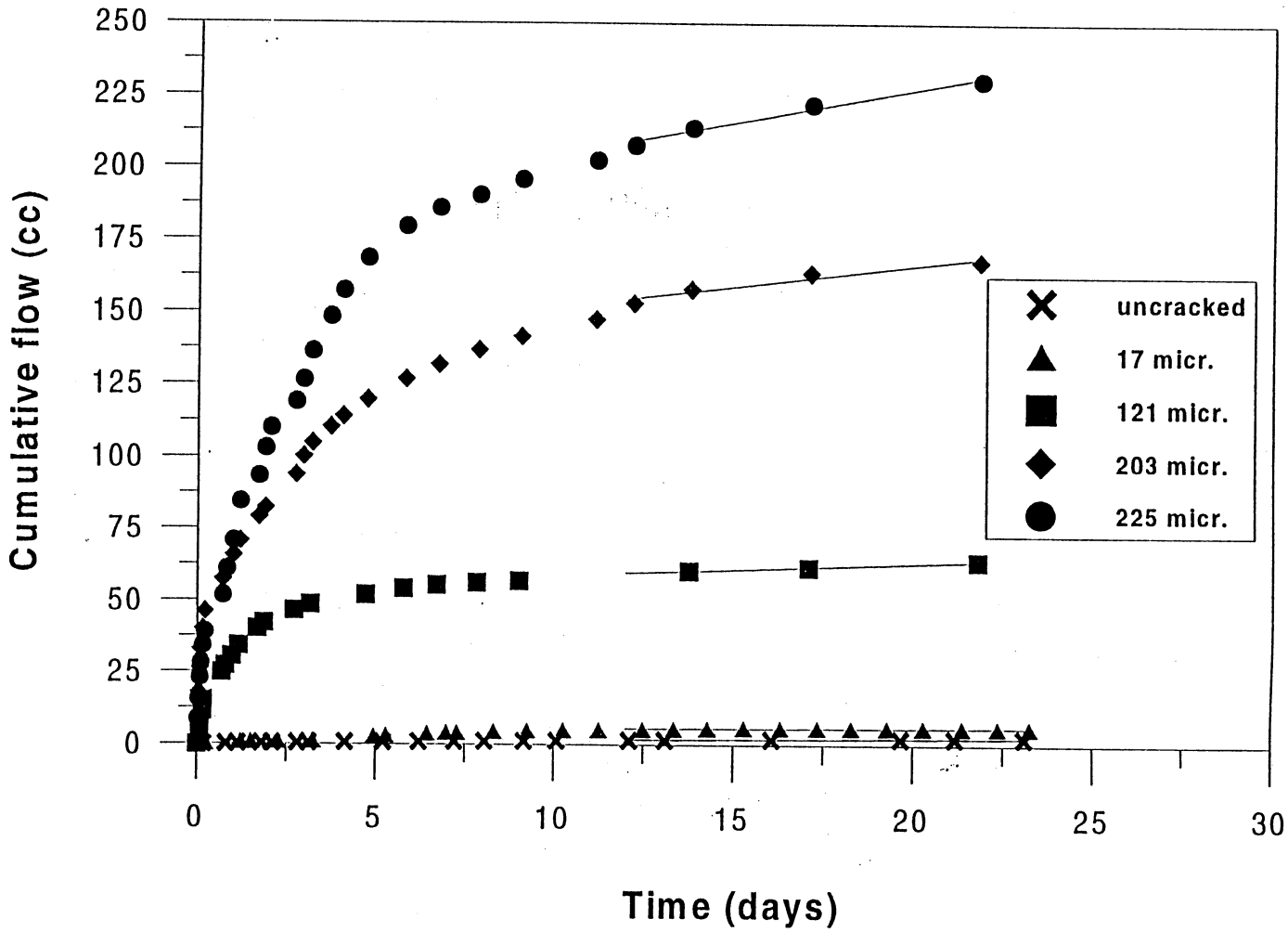

Figure 6. Dependence of cumulative flow with cracking. NSC, 25 mm.

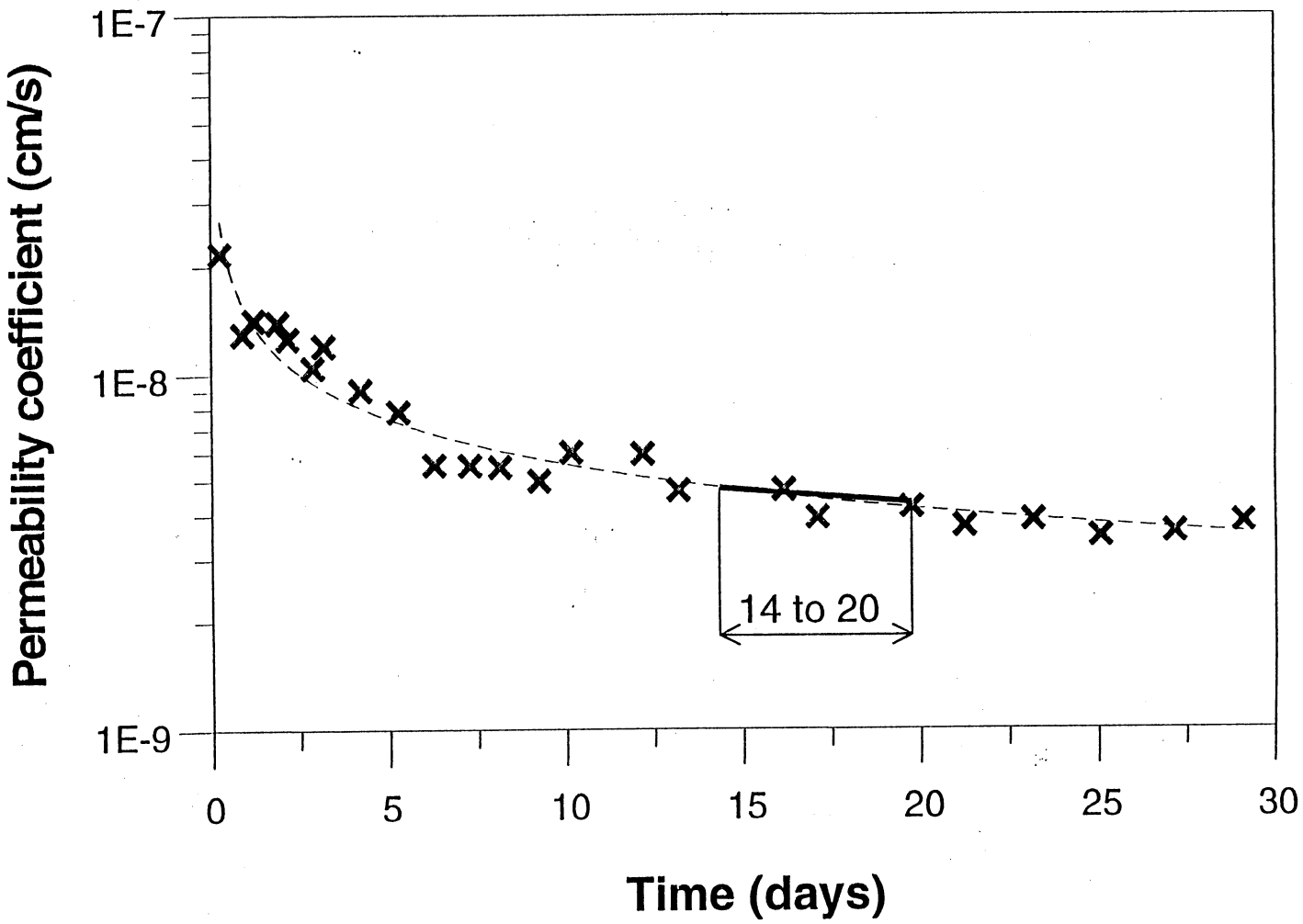

Figure 7. Typical permeability coefficient curve in time. NSC, 50 mm, COD 53 microns.

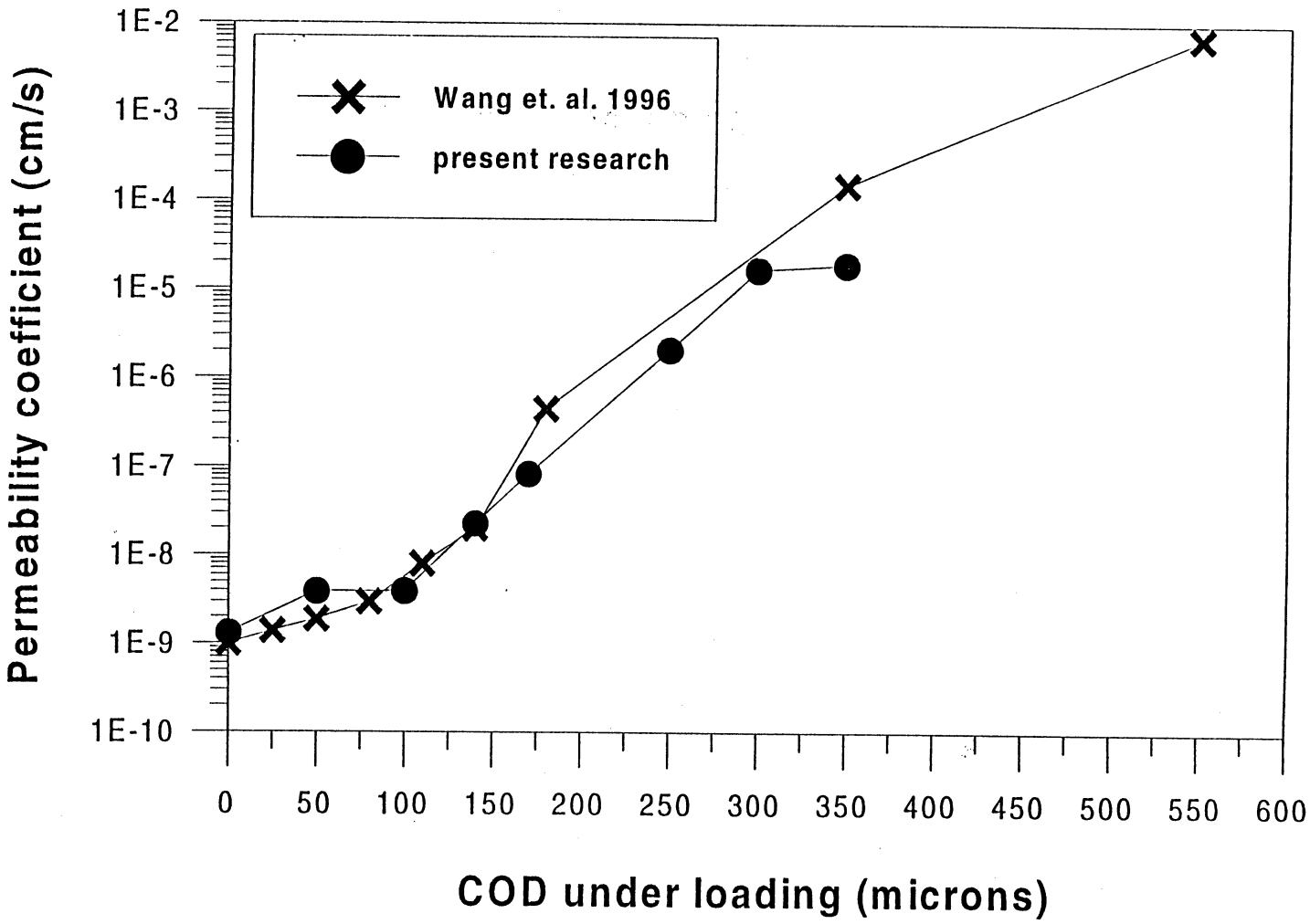

Figure 8. Cracking effect on permeability. NSC, 25 mm.

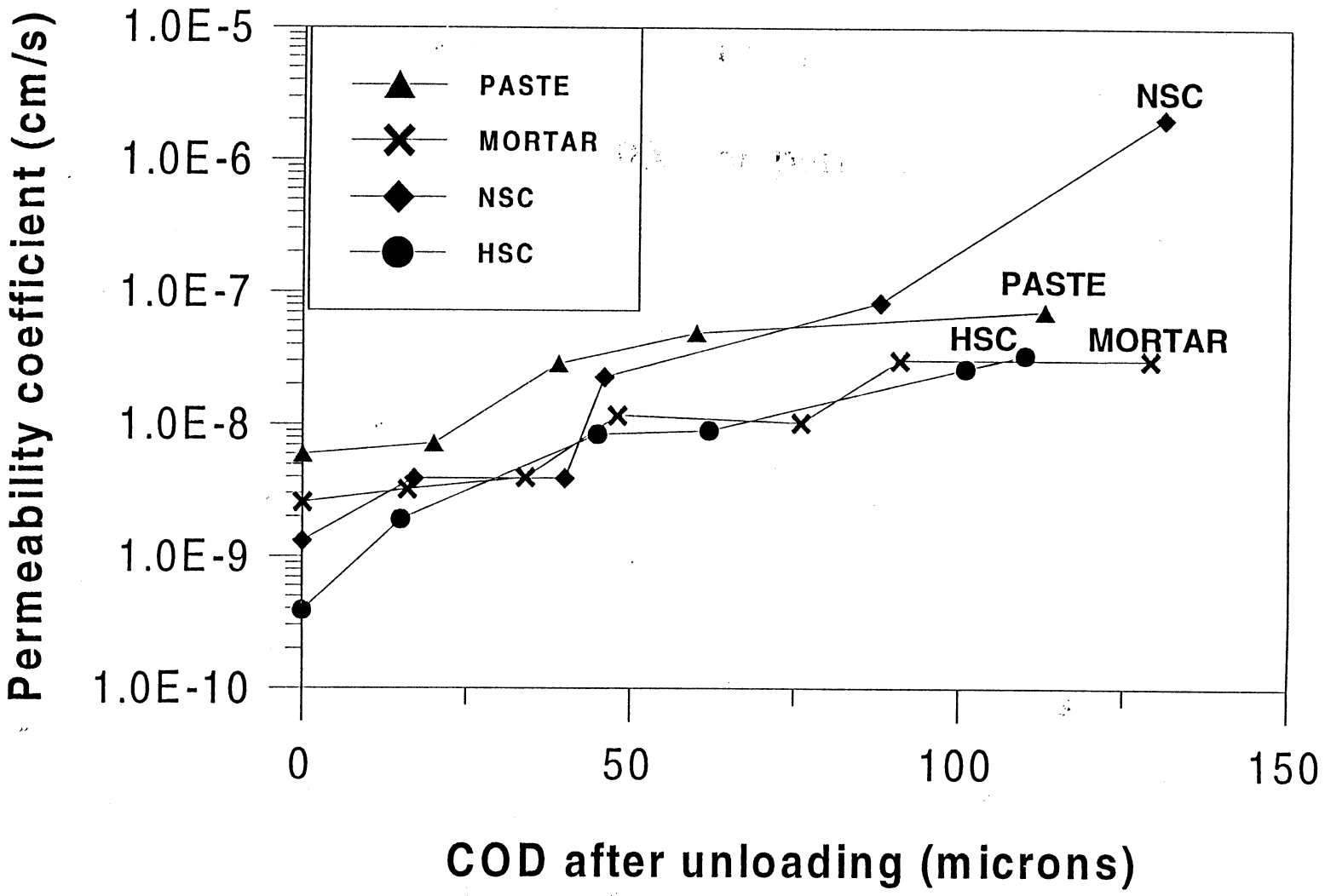

Figure 9. Material effect on permeability, 25 mm.

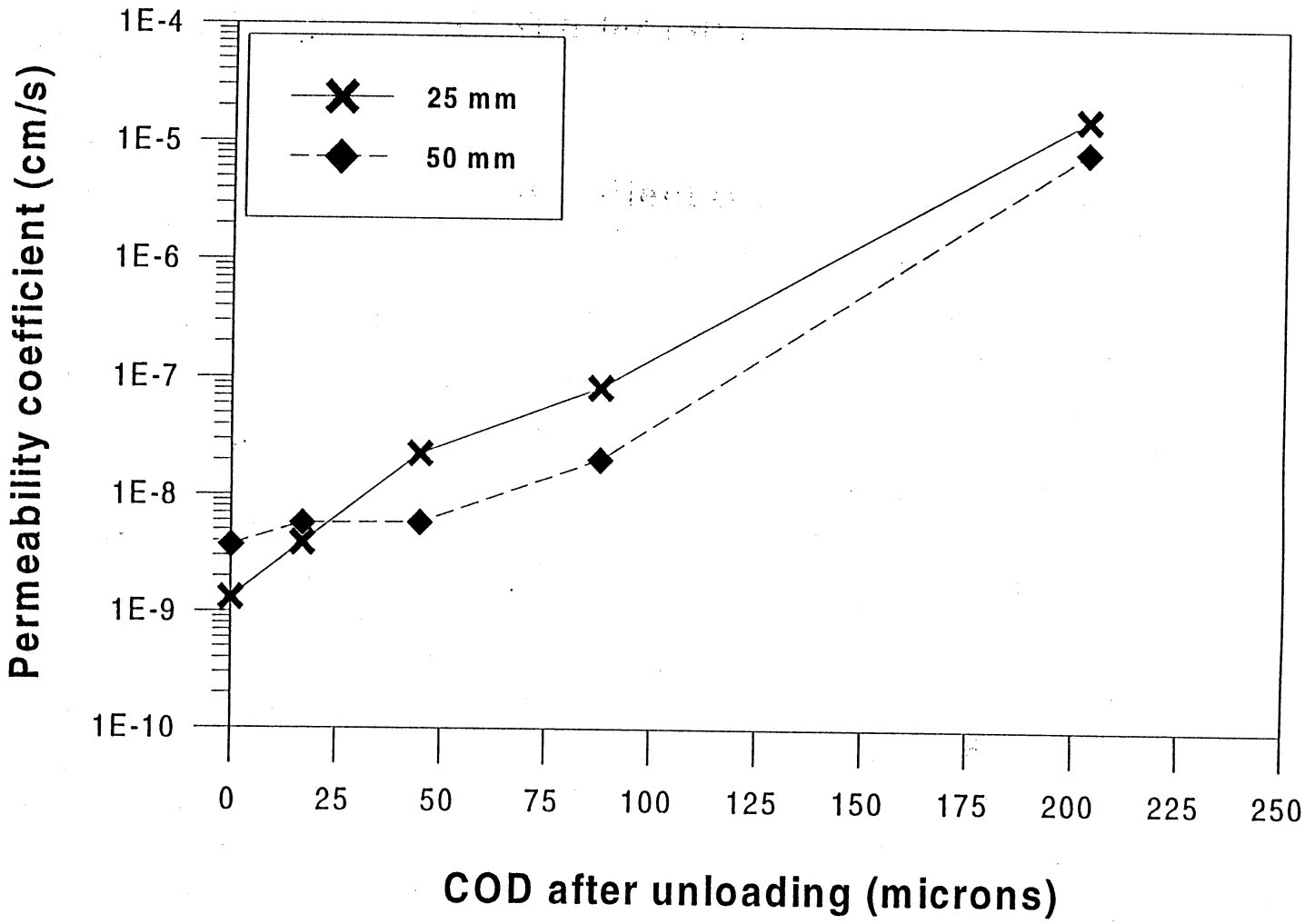

Figure 10. Thickness effect on permeability, NSC.

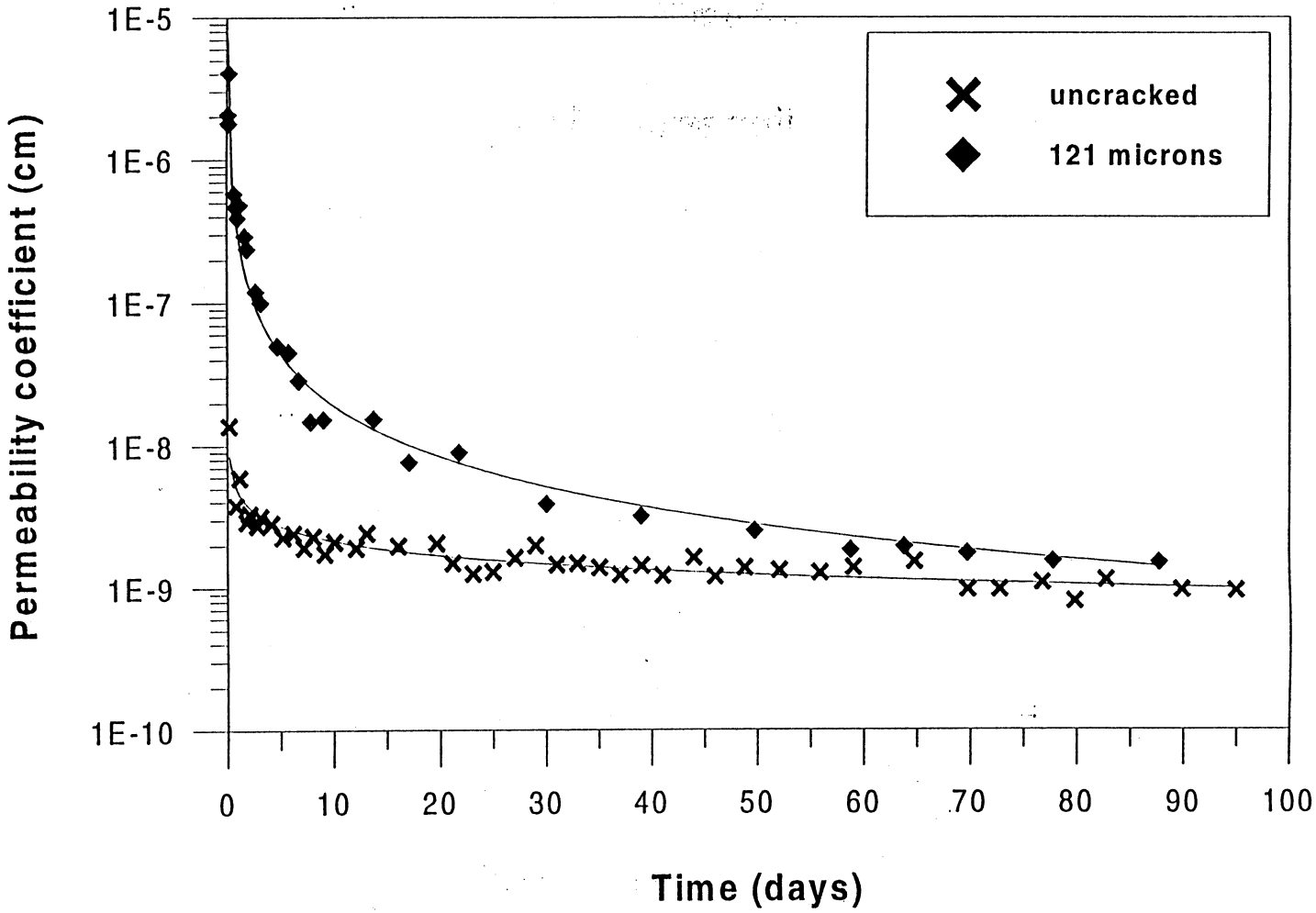

Figure 11. Dependence of permeability coefficient with time. NSC, 25 mm.

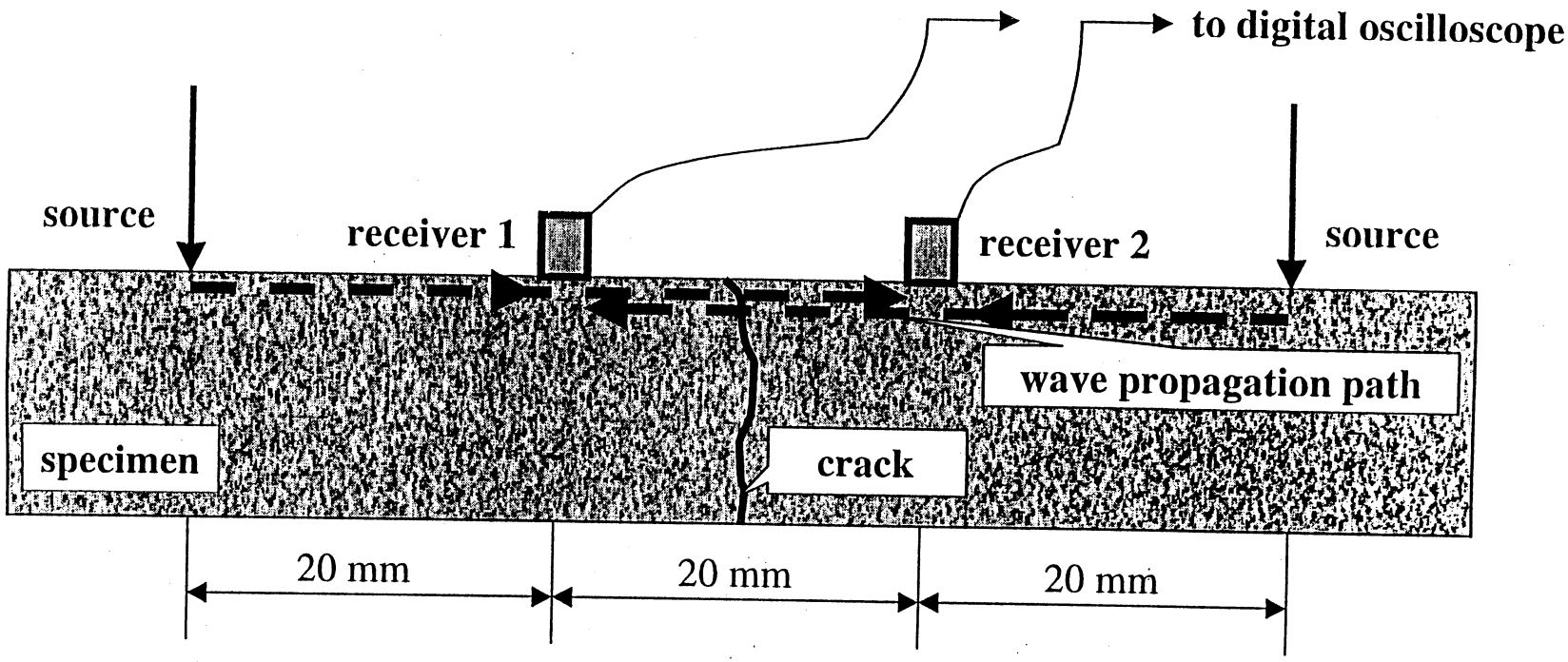

Figure 12. One-sided attenuation measurement experimental setup.

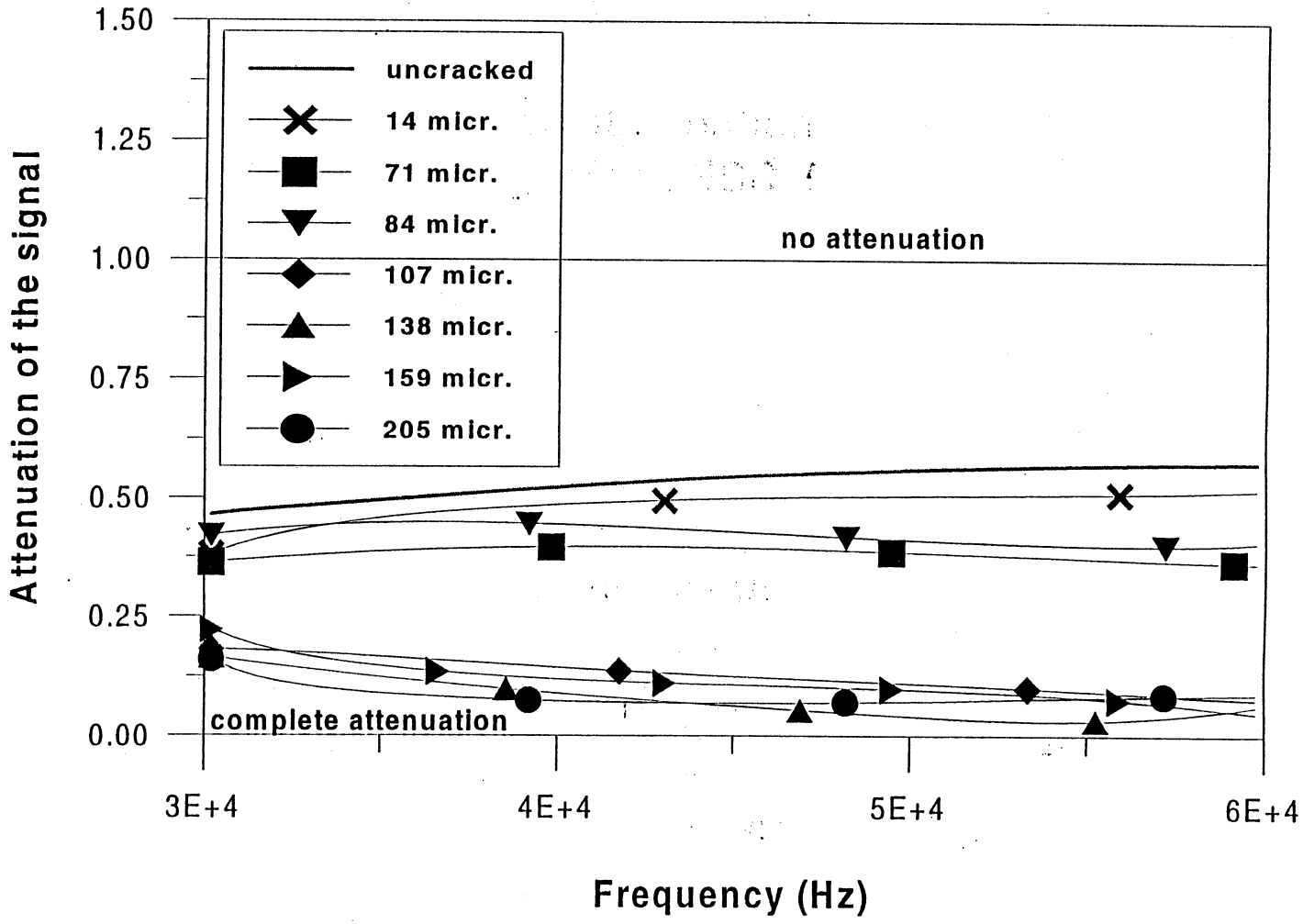

Figure 13. One-sided attenuation measurement, cracking effect, NSC, 50 mm.

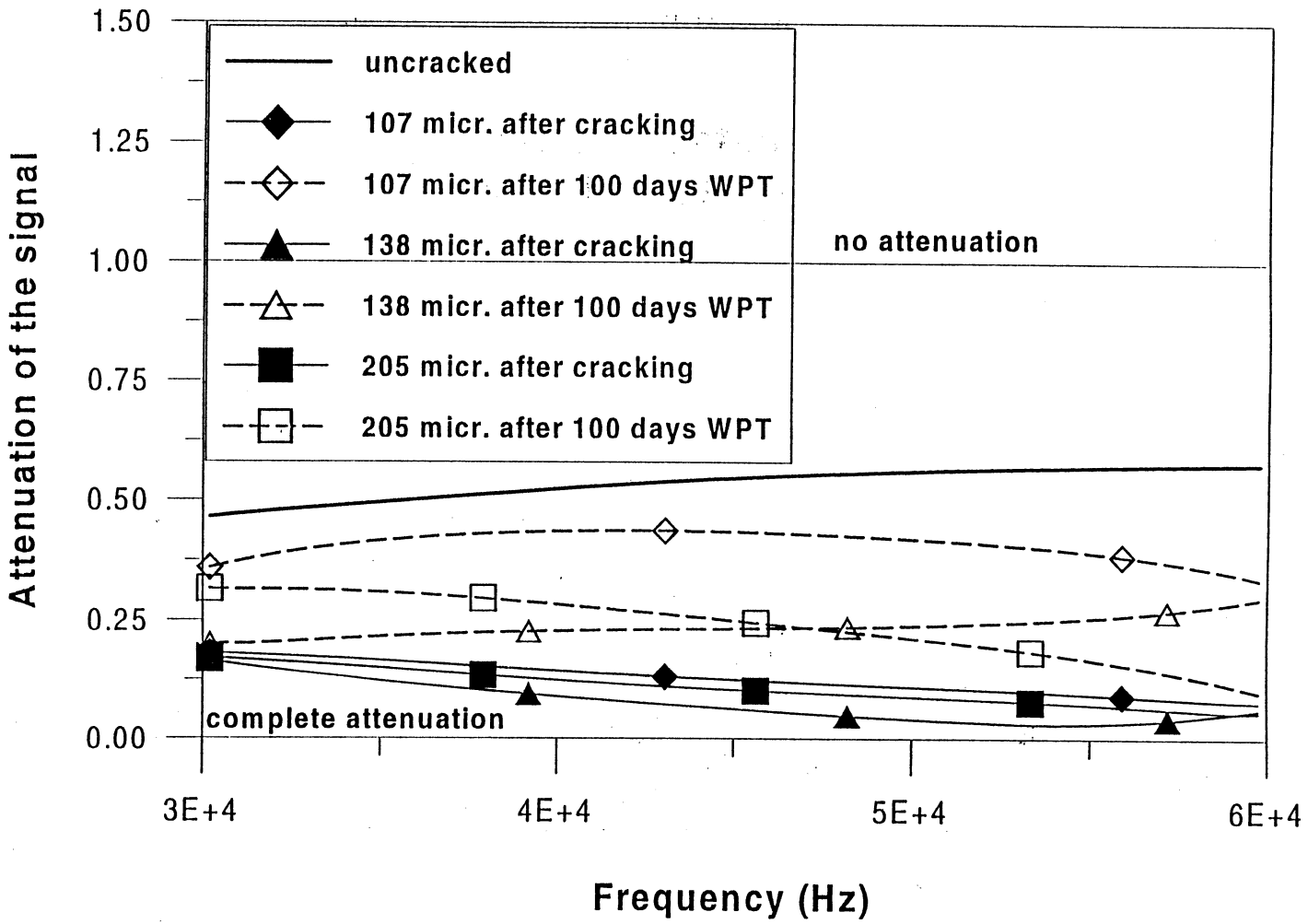

Figure 14. One-sided attenuation measurement, WPT effect, NSC, 50 mm.